STEM CELLS AND DEVELOPMENT
Volume 25, Number 11, 2016

DOI: 10.1089/scd.2016.0032

# Identification of CD90 as Putative Cancer Stem Cell Marker and Therapeutic Target in Insulinomas

Floryne O. Buishand,[1] Ger J.A. Arkesteijn,[2] Laurien R. Feenstra,[1] Claire W.D. Oorsprong,[1] Margiet Mestemaker,[1] Achim Starke,[3] Ernst-Jan M. Speel,[4] Jolle Kirpensteijn,[1] and Jan A. Mol[1]

The long-term prognosis after surgical resection of malignant insulinoma (INS) is poor. Novel adjuvant therapies, specifically targeting cancer stem cells (CSCs), are warranted. Therefore, the goal of this study was to characterize and target putative INS CSCs. Using fluorescence-activated cell sorting, human INS cell line CM and pancreatic carcinoid cell line BON1 were screened for the presence of stem cell-associated markers. CD90, CD166, and GD2 were identified as potential CSC markers. Only $CD90^+$ INS cells had an increased tumor-initiating potential in athymic nude mice. Anti-CD90 monoclonal antibodies decreased the viability and metastatic potential of injected cells in a zebrafish embryo INS xenograft model. Primary INS stained positive for CD90 by immunohistochemistry, however also intratumoral fibroblasts and vascular endothelium showed positive staining. The results of this study suggest that anti-CD90 monoclonals form a potential novel adjuvant therapeutic modality by targeting either INS cells directly, or by targeting the INS microenvironment.

## Introduction

Insulinomas (INS), consisting of tumor cells with a β-cell phenotype, are the most common functioning pancreatic neuroendocrine tumors (pNETs) in humans [1]. Most INS are small (diameter <2 cm), solitary tumors, which are treated effectively by surgical excision. However, 10%–15% of human INS metastasize to regional lymph nodes and the liver, and these are referred to as malignant INS [2]. Surgical excision of malignant INS is rarely complete and malignant INS generally respond poorly to traditional chemotherapeutic agent regimens. Therefore, recurrence is likely, leading to decreased survival times in affected individuals. Reported 10-year survival rate is <20% for malignant INS, and median survival is <2 years [3,4].

Cancer stem cells (CSCs) are considered unique subpopulations inside the heterogeneous cell population of a tumor, which are solely responsible for tumor initiation, metastasis, and recurrence [5]. The origin of CSCs is highly debated. CSCs could either derive from (i) normal stem cells that undergo malignant transformation, or from (ii) mature differentiated cells that dedifferentiate toward a stemness state [6]. Regarding the first theory, the presence and origin of stem cells in the adult pancreas remains unverified and strongly debated. The early endocrine progenitor cell in the embryonic islet lineage developmental pathway has been extensively characterized, and is known for its expression of transcription factors *NGN3*, *NKX6.1*, *PDX1,* and *NKX2.2* [7]. However, no consensus has been obtained on the location of adult pancreatic stem cells that give rise to β-cells, as conflicting in vivo data suggest that they are either present in the ductal, acinar, or islet compartment of the pancreas [8]. The occurrence of epithelial–mesenchymal transition (EMT) fits with the second theory on the origin of CSCs, and has been implicated to induce CSC generation and epithelial tumor progression [9,10]. EMT has also been implicated as a critical step in tumorigenesis of pNETs [11].

To improve the prognosis for patients with malignant INS, the development of novel CSC-targeting adjuvant therapies might be of clinical importance. Until now, however, CSC-like cells have not been convincingly identified and isolated from pNETs. Indirect evidence comes from a number of observations. Several groups have reported the activation of different embryonic cell signaling pathways (ie, Notch and Hedgehog) in gastroenteropancreatic NETs, which can be perceived as indirect evidence for the existence of pNET CSCs [12]. Furthermore, the occurrence of cells with insular–ductular differentiation in an INS liver metastasis of a patient with a purely endocrine primary INS has been implicated to support the concept that the endocrine and exocrine components have a

[1]Faculty of Veterinary Medicine, Department of Clinical Sciences of Companion Animals, Utrecht University, Utrecht, The Netherlands.
[2]Flow Cytometry Unit, Faculty of Veterinary Medicine, Division of Immunology, Utrecht University, Utrecht, The Netherlands.
[3]Department of Surgery, Lukas Krankenhaus GmbH, Neuss and Insulinoma and GEP-NET Tumor Center Neuss-Dusseldorf, Neuss, Germany.
[4]Department of Pathology, GROW-School for Oncology and Developmental Biology, Maastricht University Medical Center, Maastricht, The Netherlands.

common stem-cell origin [13]. Moreover, in a previous study we have demonstrated that canine INS contain a small population of amphicrine cells with a stem cell phenotype, expressing both endocrine hormones as well as exocrine enzymes [14]. Yet, pNETs might arise from different cells of origin. Recently it was demonstrated that gene expression profiles of human and murine adenomatous pancreatic islet tumors were closely related to mature β-cells, whereas less-differentiated ''metastasis-like primary'' pNETs more closely resembled β-cell precursors [15].

The goal of the current study was to identify a druggable marker for putative INS CSCs using human pNET cell lines. CD90 demonstrated to be such a marker, as CD90-positive INS cells demonstrated a more tumorigenic behavior in vivo compared with CD90-negative INS cells. CD90 is a glycosylphosphatidylinositol (GPI)-anchored glycoprotein that has been correlated with the tumorigenicity of hepatocellular carcinoma, esophageal cancer, glioma, and lung and breast cancers [16–20]. On top of that, through binding to αvβ3 integrin, CD90 has been implicated to facilitate metastasizing behavior in melanomas, by establishing an intimate connection between melanoma cells and activated endothelium [21]. Therefore, this study also investigated whether the use of an anti-CD90 monoclonal antibody (mAb) could inhibit tumor formation and metastasis in a zebrafish embryo xenograft model. Finally, CD90 immunohistochemical expression patterns were investigated using sections of human INS and adjacent normal pancreas.

## Materials and Methods

### Cell culture

The human INS cell line CM was cultured in RPMI-1640 (Gibco) supplemented with 10% fetal calf serum (FCS; GE Healthcare Life Sciences), 100 U/mL penicillin G, and 100 μg/mL streptomycin (GE Healthcare Life Sciences). CM-RED cell line, stably expressing fluorescent DsRed, was obtained by cotransfecting CM with a lentiviral Phage2-EF1aFull-Dsred Express-IRES-PuroR-Loxp plasmid. CM-RED was cultured in RPMI-1640 supplemented with 10% FCS and 1 μg/mL puromycin (Sigma-Aldrich). The human pancreatic carcinoid cell line BON1 was cultured in Dulbecco's modified Eagle's Medium/F12 (Gibco) supplemented with 10% FCS, 100 U/mL penicillin G, and 100 μg/mL streptomycin. Cells were passaged on reaching 70%–80% confluence.

To select for chemoresistant CM and BON1 cells, $5 \times 10^6$ cells were plated in Greiner T-75 cell culture flasks (Sigma-Aldrich). After 24 h 10 μg/mL doxorubicin was added to the medium. Cells that survived after 72 h of doxorubicin incubation were considered to be chemoresistant. All cells were cultured at 37°C in a humidified 5% $CO_2$ incubator.

### Cell surface marker screening

CM cells were characterized using BD Lyoplate Human Cell Surface Screening Panel (BD Biosciences; cat. 560747), which contains 242 monoclonal antibodies and corresponding isotype controls. The assay was performed according to the manufacturer's protocol. Screening of the cells was performed using a BD FACS Canto II flow cytometer with high-throughput screening 96-well plate loader. Data were analyzed by BD FACSDiva software version 7.0. Suitable cell surface markers were selected for verification and further experiments based on three criteria: (i) 5%–20% of the analyzed cells stained positive; (ii) positive cells were identified as a distinct subpopulation, separated from the main population of cells on FACS plots; (iii) PubMed search identified that the marker had already been associated to a CSC phenotype and EMT.

### Fluorescence-activated cell sorting

CM and BON1 cells were dissociated from cell cultures using TrypLE Express (Life Technologies). After washing the cells with Hank's Balanced Salt Solution (HBSS; Gibco), cells were filtered through 40 μm cell strainers and single cells were resuspended in BD Pharmigen Stain Buffer [fetal bovine serum (FBS; BD Biosciences)] containing 5 mM ethylenediaminetetraaceticacid (EDTA). Phycoerythrin (PE)-conjugated CD90 (BD Biosciences; cat. 555596), CD166 (BD Biosciences; cat. 559263), or disialoganglioside GD2 (BD Biosciences; cat. 562100) antibodies were added and the cells were incubated for 45 min on ice in the dark. After washing twice, cells were resuspended in FBS +5 mM EDTA. Samples were either analyzed using a BD/Canto Flow Cytometer, or sorted using a BD/Cytopeia Influx Flow Cytometer. The PE-conjugated antibodies were excited at 561 nm, and the emitted fluorescence was detected through the FL7 channel. The flow cytometers were set using isotype controls. All experiments included negative controls without antibodies and cells were gated by forward and sideward scatter to eliminate debris. Fluorescence-activated cell sorting (FACS) data were analyzed using FlowJo 7.6 software.

### RNA extraction and cDNA synthesis

Total RNA from CM and BON1 cells, cultured with or without doxorubicin, was extracted using the RNeasy Mini Kit (Qiagen). An on-column DNase treatment was included to prevent contamination of the samples with genomic DNA. RNA concentrations were measured using spectrophotometry (NanoDrop ND-1000; Isogen Life Sciences) and 2 μg total RNA was reverse transcribed in a total reaction volume of 40 μL to create enough volume of cDNA (the iScript cDNA Synthesis Kit; Bio-Rad). Reactions without reverse transcriptase enzyme were performed for all samples as negative controls.

### Quantitative real-time polymerase chain reaction

The mRNA expression of *CD90*, two EMT markers, and eight pancreas progenitor genes was evaluated by quantitative real-time polymerase chain reaction (qPCR). Primers were designed using PerlPrimer v 1.1.14 software (Supplementary Table S1; Supplementary Data are available online at www.liebertpub.com/scd). Sequencing confirmed specificity of the amplicons. cDNA samples were diluted 1:10 in milliQ water, divided into aliquots, and stored at –20°C until further use. For each target gene, a master mix was prepared, using SYBR Green Supermix (Bio-Rad). qPCR was performed using a CFX384 Real-Time system C1000 touch thermal cycler (Bio-Rad), with three-step reactions (denaturation, annealing, and elongation) [22]. *HPRT*, *RPL19*, and *GAPDH* were included as endogenous reference genes. Each reaction was performed in duplicate, and efficiency

was assessed by a dilution series of pooled cDNA samples in each run. Efficiency cut-offs were 95%–105%. Omission of the reverse transcriptase reaction showed no significant contamination with genomic DNA. Normalized gene expressions were compared using the $^{2-\Delta\Delta Ct}$ method to obtain fold changes.

### *In vivo assay of tumorigenicity*

Female athymic nude mice, aged 5 weeks were purchased from Harlan Laboratories. Each mouse received four subcutaneous injections. On the right flank FACS sorted CM $CD90^+$ or $GD2^+$ cells were injected, and on the left flank FACS sorted CM $CD90^-$, or $GD2^-$ cells were injected. On the left shoulder CM cells that had run through the BD/Cytopeia Influx Flow Cytometer, but had not been sorted, were injected. Mice received either $1\times10^4$, or $1\times10^5$ cells per injection site. Negative control samples of HBSS without cells were injected on the right shoulders. Tumor formation was monitored twice weekly for a maximum of 12 weeks. Tumor volume ($V$) was measured using the equation $V=(\text{length})\times(\text{width})^2/2$. Mice were euthanized when the largest subcutaneous tumor reached 1.0 $cm^3$. The experiments were approved by the Animal Experiments Committee of Utrecht University, The Netherlands.

### *In vivo inhibitory effect of anti-CD90*

Zebrafish embryo xenograft experiments in this study were approved by the Animal Experiments Committee of Utrecht University, The Netherlands. The transgenic zebrafish line Tg(fli1:GFP) [23] (generous gift of Brant M. Weinstein, PhD, National Institute of Health) was used, and zebrafish were raised and maintained according to standard procedures [24]. Dechorionized 2 day-postfertilization zebrafish embryos were anesthetized with 0.003% tricaine (Sigma) and positioned on a 10-cm Petri dish coated with 1% agarose. Single cell suspensions of CM-RED were resuspended in 2% polyvinylpyrrolidone (Sigma-Aldrich) in HBBS (200 cells/nL) and were implanted within 1 h. Zebrafish embryos were either injected with 2 nL CM-RED cell suspension, or with 2 nL CM-RED cell suspension containing 100 ng/mL anti-CD90 mAb (Millipore; CBL415). The cell suspension was loaded into needles that were manually pulled from glass capillaries using a P-97 Micropipette Puller (Sutter Instrument). Injections into the yolk sac or in the duct of Cuvier were performed using a Pneumatic PicoPump and a manipulator (Warner Instruments). Directly after implantation, proper injection was evaluated by fluorescence microscopy. Zebrafish embryos were maintained at 33°C as a compromise between optimal temperature requirements for zebrafish and mammalian cells. Experiments were conducted in triplicate with 30–40 well-injected embryos per group. The survival rate 1 day postinjection (dpi) was >90% each time.

Embryos were fixed in 4% paraformaldehyde solution at 3 or 5 dpi. For imaging, zebrafish embryos were embedded in 1% agarose on six-well chamber slides (Ibidi). Image acquisition was performed using a Leica SPE-II–DMI4000 confocal fluorescence microscope. Images were processed and overlays were created using Leica Application Suite Advanced Fluorescence software. Localization of tumor cells and the percentage of embryos with metastases were scored. Differences in the number of zebrafish with distant metastases found were evaluated statistically using Fishers exact test, and $P<0.05$ was assumed significant.

### *Immunohistochemistry*

Paraffin-embedded blocks of 17 non-metastasized well-differentiated (WHO classification 2010 grade 1), and three metastasized and/or moderately differentiated grade 2 human INS were available from the INS and GEP-NET Tumor Center Neuss-Dusseldorf. Sections were cut at 5 μm and donated to Utrecht's Faculty of Veterinary Medicine for CD90 immunohistochemistry. Sections of normal human thymus tissue were used as positive controls, while omission of the primary antibody served as negative control. Ten out of 17 INS sections included an internal negative control, because these sections contained normal islets embedded in the normal pancreatic tissue adjacent to the INS.

Sections were deparaffinized, and treated in 10 mM citrate buffer (pH 6) for 20 min at 98°C. After rinsing in phosphate-buffered saline (PBS), sections were treated with 6% $H_2O_2$ in PBS for 5 min to block endogenous peroxidase activity. Sections were rinsed in PBS containing 0.2% Tween (PBST) and blocked for 60 min with 2% bovine serum albumin in PBST. Sections were incubated overnight at 4°C with rabbit monoclonal anti-CD90 (Abcam; ab133350) at a dilution of 1:100. After incubation, slides were washed with PBST and then incubated for 60 min with Envision anti-rabbit (DAKO). After another wash with PBST, the antigen–antibody reaction was visualized following addition of 3,30-diaminobenzidine. Slides were counterstained with Hematoxylin. Sections were dehydrated through ascending ethanol series and xylene and mounted with coverslips over VectaMount permanent mounting medium.

CD90 positivity (percentage positive nuclei) was scored in tumor cells, intratumoral fibrous bands, and vascular endothelium.

## Results

### *Cell surface marker screening*

Expression of cell surface markers on CM INS cells was evaluated by FACS analysis of cells after incubation with a panel of 242 different antibodies (Lyoplate; BD Biosciences) (Fig. 1; Supplementary Table S2). Markers of interest for further experiments were selected based on the following criteria:

- Distinct positive subpopulation (5%–20%) of cells on FACS plot.
- Positive hits on PubMed Search, using as input a combination of ''cell surface marker of interest,'' with ''EMT,'' and ''cancer stem cells.''

Only three markers met the inclusion criteria, being: CD90 (16% positive cells), CD166 (15% positive cells), and disialoganglioside (GD2) (13% positive cells). To validate the screening results, flow cytometry on CM was performed using PE-conjugated antibodies against CD90, CD166, and GD2. Similar percentages of positive cells were found compared with the Lyoplate results for CD90 and GD2 (Fig. 2), whereas >20% positive cells were found for CD166. Flow cytometry on BON1 cells was also performed

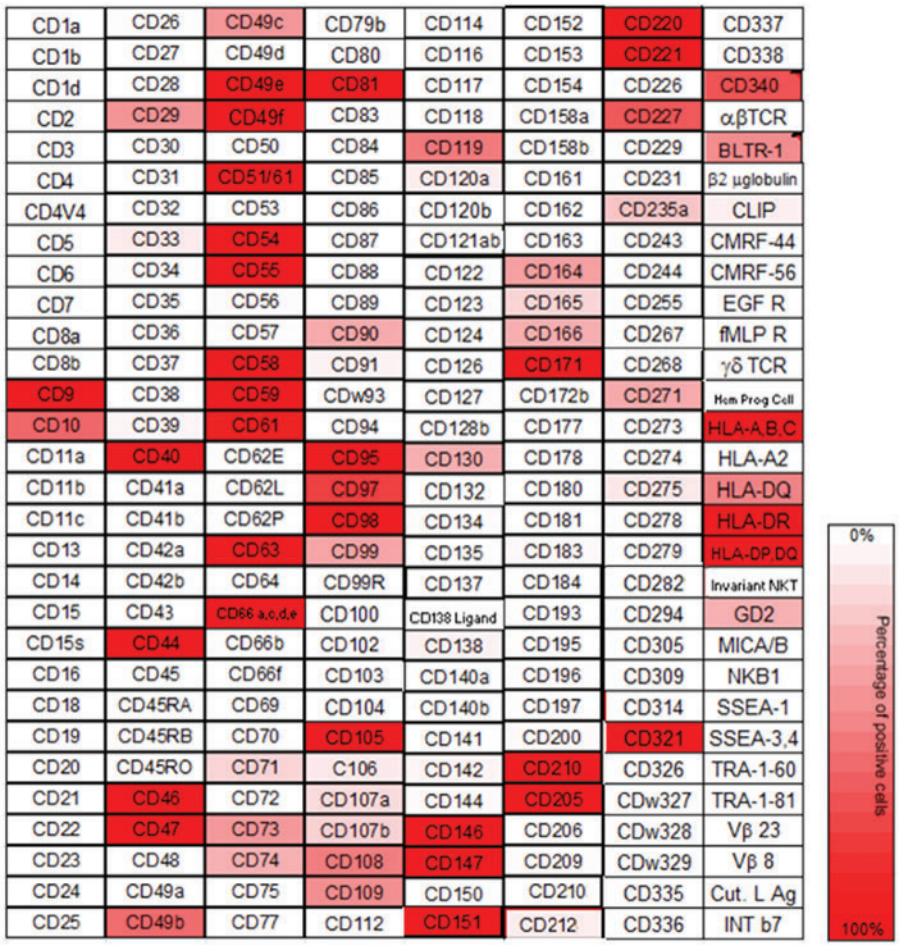


**FIG. 1.** Heat map of cell surface marker expression by insulinoma cell line CM. For mAb clones and abbreviations, see www.bdbiosciences.com mAb, monoclonal antibody. Color images available online at www.liebertpub.com/scd

using PE-conjugated antibodies against CD90 and GD2, and the percentages of positive cells were $CD90^+$: 15%, and $GD2^+$: 5%.

### *Doxorubicin-induced gene expression changes*

Relative cell viability after 72 h doxorubicin treatment, measured by MTT assays, was 20% for CM and 28% for BON1 in comparison to untreated controls. Normalized fold changes of gene expression of doxorubicin-resistant versus nonresistant cells were measured (Table 1). Expression analysis of genes involved in the differentiation of endocrine pancreas cells (Supplementary Fig. S1) revealed that *CD90*, *NKX6.1*, *SNAI1*, and *SOX17* were upregulated ≥2-fold in doxorubicin-resistant cells of both cell lines. *GATA4*, *NEUROG3*, *NKX2.2*, *PAX4*, and *PDX1* were uniquely ≥2-fold upregulated in doxorubicin-resistant CM cells, while *TWIST1* was uniquely ≥2-fold upregulated in doxorubicin-resistant BON1 cells.

### *In vivo tumorigenicity*

Since pNETs (including INS) and carcinoid tumors should be treated as separate classes of neuroendocrine tumors, reflected by their difference in clinical behavior and gene expression [25], in scope of our study goal, we decided to use the CM cell line for in vivo experiments. CM is a true INS cell line, while BON1 is a pancreatic carcinoid cell line, and the gene expression of CM-doxorubicin-resistant cells better resembles fetal β-cells, compared with doxorubicin-resistant BON1 cells (Table 1; Supplementary Fig. S1).

None of the mice that received $1\times10^4$ CM cells per injection site developed tumors (Table 2). Six out of eight mice that received $1\times10^5$ $CD90^+$ cells, developed tumors at the marker positive injection spot within 2–4 weeks, whereas none of the mice that received $1\times10^5$ $GD2^+$ cells developed a tumor at that injection site (Fig. 3). After 6 weeks 1/8 mice from the CD90 group developed a tumor at the unsorted cell spot, and after 7 weeks 2/4 mice from the GD2 group developed tumors at the unsorted cell spot.

### *In vivo inhibitory effect of anti-CD90*

With respect to the 3R principle (reduction, refinement, replacement) of animal use in biomedical research [26], and because of their relative easy way of use, we decided to use zebrafish embryos for further in vivo experiments. Zebrafish embryos were injected with DsRed-labeled CM cells (CM-RED) either into the yolk sac or directly into the circulation using the duct of Cuvier. Cells were injected in the absence or presence of an anti-CD90 mAb.

In the majority of zebrafish embryos, that is 80%, cells injected into the yolk sac further grew out as major tumor clumps within the yolk sac (Fig. 4A), the remaining 20%

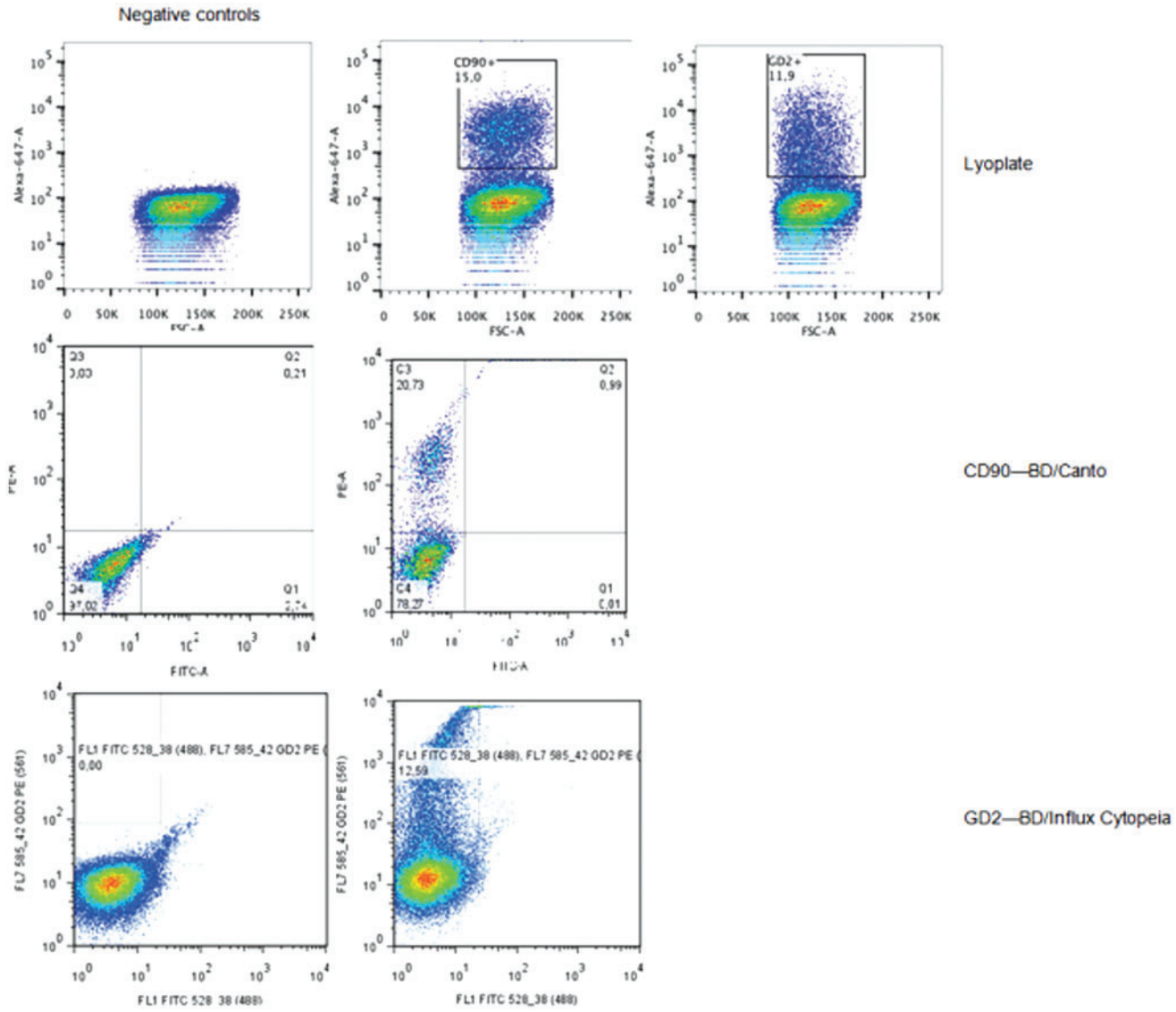


**FIG. 2.** Flow cytometry plots for markers CD90 and GD2 in insulinoma cell line CM. Lyoplate screening results were validated on both BD/Canto and BD/Influx Cytopeia flow cytometer. Color images available online at www.liebertpub.com/scd

demonstrated small tumor clumps. The addition of anti-CD90 resulted in the presence of smaller tumor clumps in 35%, or only single cells in 65% of the zebrafish embryos (Fig. 4B). Without anti-CD90, yolk sac-injected cells also formed metastases in 13% of the injected embryos at 3 dpi until 40% at 5 dpi, whereas no metastases were found in the presence of anti-CD90. Injection directly into the circulation, in which a high load of tumor cells is present in the circulation, resulted in a higher frequency of metastases (44% at 3 dpi, and 68% at 5 dpi), but especially at 5 dpi significantly less metastases were found in embryos injected with cells together with anti-CD90 (Fig. 4C–E).

### *Immunohistochemistry*

All three moderately differentiated INS stained positive for CD90, whereas 10/17 well-differentiated INS stained positive for CD90 (Fig. 5A). No CD90 positivity was observed in normal pancreatic endocrine and exocrine cells on 10 INS sections that included normal pancreatic tissue

Table 1. Normalized Fold Changes of Gene Expression of Doxorubicin-Resistant Versus Nonresistant Pancreatic Neuroendocrine Tumor Cells

| *Cell line* | *CD90* | *GATA4* | *NEUROG3* | *NKX2.2* | *NKX6.1* | *PAX4* | *PDX1* | *SNAI1* | *SOX9* | *SOX17* | *TWIST1* |
|---|---|---|---|---|---|---|---|---|---|---|---|
| CM | 2.0 | 2.0 | 323.6 | 3.6 | 25.2 | 109.7 | 2.7 | 5.5 | 1.7 | 5.5 | 1.5 |
| BON1 | 6.6 | 1.8 | 1.6 | 0.5 | 6.5 | 1.6 | 1.0 | 8.5 | 0.9 | 75.9 | 19.0 |

Table 2. Overview of the Number of Mice that Developed Tumors at Specific Injection Sites

| *Group* | *Marker-positive spot* | *Marker-negative spot* | *Unsorted cells spot* | *Negative control spot* |
|---|---|---|---|---|
| $1\times10^4$ cells—CD90 | 0/3 | 0/3 | 0/3 | 0/3 |
| $1\times10^5$ cells—CD90 | 6/8 | 0/8 | 1/8 | 0/8 |
| $1\times10^4$ cells—GD2 | 0/3 | 0/3 | 0/3 | 0/3 |
| $1\times10^5$ cells—GD2 | 0/4 | 0/4 | 2/4 | 0/4 |

(Supplementary Fig. S2). Only some fibroblasts in the normal pancreatic tissue showed some faint cytoplasmic staining. Intratumoral fibrous bands stained positive in all INS with moderate differentiation, whereas 12/15 well-differentiated INS containing fibrous bands demonstrated $CD90^+$ stroma (Fig. 5B). Two out of three INS with moderate differentiation contained vascular endothelium, based on the presence of erythrocytes inside endothelium-lined lumens (Fig. 5C). In both cases vascular endothelium stained intensely positive for CD90. Vascular endothelium was present in 8/17 well-differentiated INS, however, no positive endothelium was observed in any of these cases.

## Discussion

FACS screening and subsequent validation of the INS cell line CM identified CD90 and GD2 as potential CSC markers. These markers were also shown to be expressed on the pancreatic carcinoid cell line BON1 indicating that these markers may be more generalized for pNETs. However, from our nude mice xenograft model it followed that only $CD90^+$ INS cells demonstrated an enhanced tumor-initiating capability, whereas $GD2^+$ INS cells did not possess a growth advantage over unsorted INS cells. At 7 weeks 2/4 mice from the GD2 group developed a tumor at the unsorted cell spot, whereas only 1/8 from the CD90 group developed a tumor at that spot. Probably, more mice from the CD90 group would have eventually developed a tumor at the unsorted cell spot. However, most mice from this group had already reached the human endpoint before 7 weeks, because their $CD90^+$ tumors that started growing at 2 weeks measured 1.0 $cm^3$ within 4 weeks.

CD90, also known as Thy-1, is a 25–37 kDa GPI-anchored glycoprotein, which is expressed on membranes of fibroblasts, neurons, activated microvascular endothelial cells, and mesenchymal and hepatic stem cells [27–30]. Although CD90's exact function is currently unknown, it has been implicated to have a significant role in cellular adhesion and migration, regulating cell–cell and cell–matrix interactions [31]. Besides its expression on certain normal cell types, CD90 has been described as a CSC marker in various malignancies, such as hepatocellular carcinoma, esophageal cancer, glioma, and lung and breast cancers [16–20]. In this study, we demonstrated for the first time that CD90 also appears to be a potential CSC marker for INS, because $CD90^+$ CM cells had an enhanced in vivo tumor-initiating capability. More research is needed to determine whether the link between CD90 expression and increased tumorigenicity in INS cells is a causative or merely an associative link. For instance, Jiang et al. demonstrated that expression of CD90 on gastric CSCs was correlated with ERBB2 expression, and that trastuzumab (Herceptin, mAb against ERBB2) targeted gastric CSCs characterized by the CD90 phenotype [32]. On the other hand, another study, while still mainly descriptive, demonstrated that transfection of a liver cancer cell line with a CD90 expression vector paralleled a decrease in E-cadherin expression and thereby increased migration and invasion of the liver cancer cells, implying a causal effect of CD90 expression and increased tumorigenicity [33]. Most recent and elegant evidence on the signaling network of CD90 comes from Chen et al., who demonstrated that the signal axis of CD90-integrin-mTOR/AMPK-CD133 is critical for promoting liver carcinogenesis [34]. Future studies should focus on knockdown of CD90 in

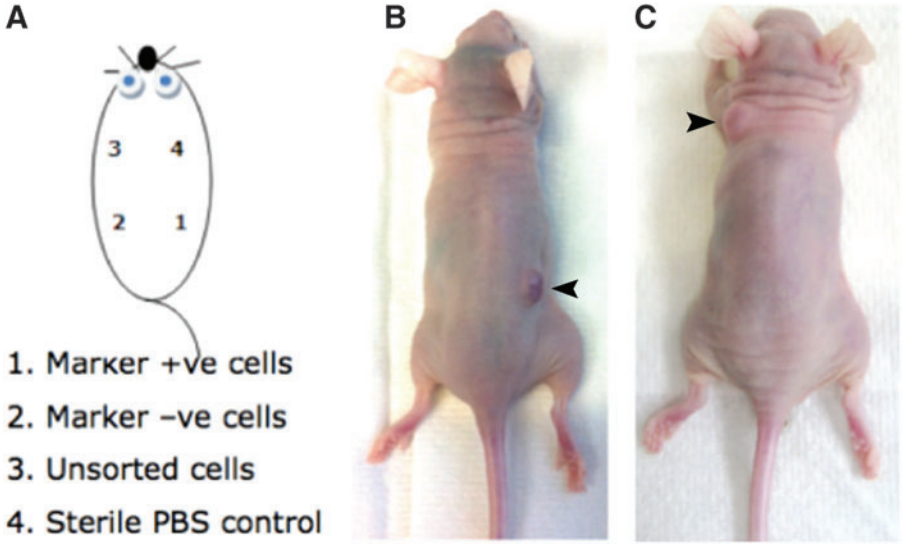


**FIG. 3.** Tumorigenicity assays in athymic nude mice. **(A)** Schematic overview of cell populations injected at specific subcutaneous locations. **(B)** A representative mouse from the CD90 group displaying a tumor grown from CD90+ cells (marked with *arrowhead*). **(C)** A representative mouse from the GD2 group displaying a tumor grown from unsorted CM cells (marked with *arrowhead*). Color images available online at www.liebertpub.com/scd

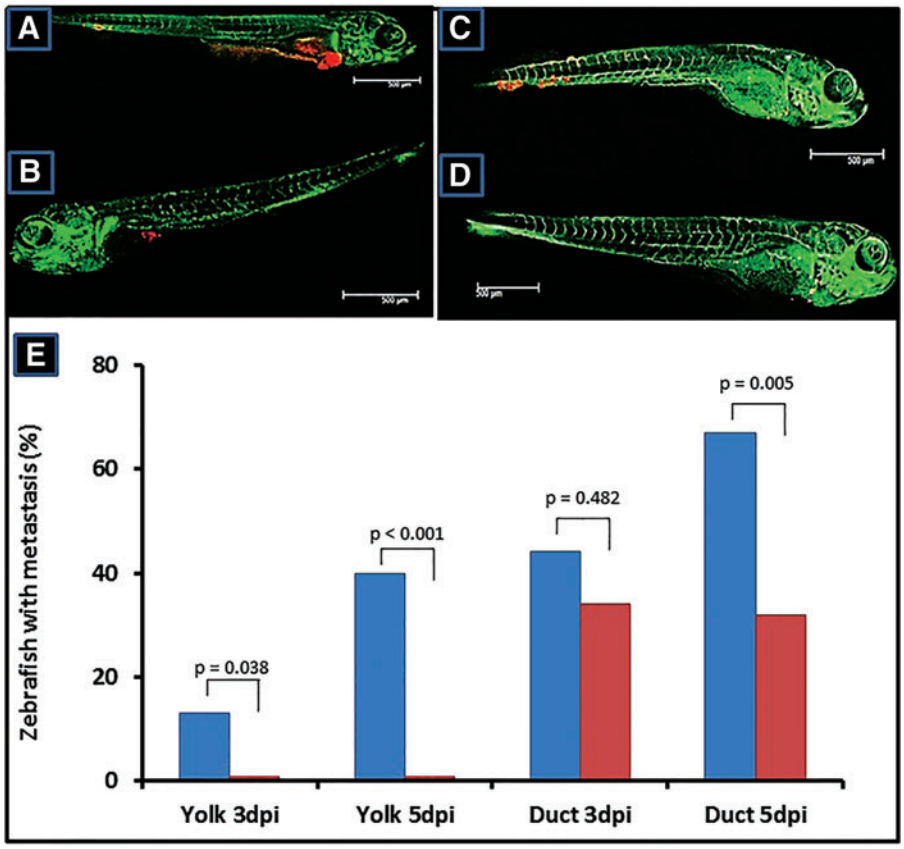


**FIG. 4.** Examples of zebrafish embryo insulinoma xenografts. **(A)** Zebrafish embryo injected with CM-*RED* cells into the yolk sac occupy a major part of the yolk sac and show distant metastases, whereas **(B)** in the presence of anti-CD90 mAb embryos display only small tumor clumps in the yolk sac and no metastases. **(C)** Direct injection within the duct of Cuvier results in distant metastases, whereas **(D)** in the presence of anti-CD90 mAb less and smaller metastases are present especially at day 5 postinjection. **(E)** Statistical evaluation of embryos with distant metastases after injection of CM-*RED* cells into the yolk sac or duct of Cuvier at day 3 and 5 postinjection. Color images available online at www.liebertpub.com/scd

INS cells using silencing RNA to study its effect on proliferation, apoptosis, and three-dimensional tumor sphere-forming capability.

*CD90* mRNA was upregulated both in doxorubicin-resistant CM and BON1 cells, however the upregulation was >3-fold greater in BON1 compared with CM. At the same time, BON1 doxorubicin-resistant cells had a higher upregulation of EMT markers *SNAI1* and *TWIST*, and early endocrine progenitor cell marker *SOX17*, whereas CM doxorubicin-resistant cells had a higher upregulation of late fetal β-cell progenitor cell markers *NKX2.2*, *NKX6.1*, *NEUROG3*, and *PAX4*. The difference in progenitor marker expression can be explained by the fact that the CM cell line has a β-cell phenotype [35], whereas BON1 cells originate from a pancreatic carcinoid, lacking β-cell characteristics [36]. Regarding the upregulation of EMT markers, previously it has been described that chemoresistance to doxorubicin induces EMT in colon cancer and lung cancer cells [37,38]. Furthermore, in several tumor types, including pancreatic adenocarcinoma (PDAC), a link has been described between CSCs and EMT [39]. Although it is difficult to determine which event occurs first, a likely explanation is that EMT contributes to the establishment of CSCs. EMT has been described to upregulate the expression of CD90 on breast cancer and lung cancer cells [38,40]. Furthermore, EMT has been demonstrated to occur in pNETs, since positive immunohistochemical staining of human INS and INS of Rip1tag2 mice was found for SNAI1 and TWIST [11]. Furthermore, treating the Rip1tag2 mice with SNAI1 inhibitor polyethylene glycol, led to a dramatic reduction of INS volume by 97%. Taken together, the parallel enhanced expression of *CD90* with *SNAI1* and *TWIST* may support the concept that part of the INS cells undergoes EMT resulting in $CD90^+$ cells with CSC characteristics. Considering that genes associated to EMT have been reported to be upregulated in less differentiated ''metastasis-like primary'' pNETs versus adenomatous pancreatic islet tumors, this might underline that CD90 could be an additional marker for ''metastsis-like primary'' pNET cells [15]. Targeting either $CD90^+$ INS cells directly, or the EMT mechanism might prove a valuable adjuvant therapy for patients with INS.

The effect of targeting CD90 itself was modeled in zebrafish embryo xenografts. Coinjection of anti-CD90 mAb with CM-RED cells into the yolk sac of zebrafish embryos led to significant smaller tumors at 3 dpi compared with injection of CM-RED cells only. Also the yolk-injected cells did not result in metastatic foci in the presence of anti-CD90, whereas control cells did. Anti-CD90 mAb, apparently, reduced the viability and/or metastatic potency of CM-RED cells. Direct injection of CM-RED cells into the circulation resulted in the formation of metastases. Initially also cells injected in the presence of anti-CD90 mAb formed metastases, which may be due to the relatively high amount of CM-RED cells in the circulation. However, at 5 dpi, control cells showed a further increase, whereas in the presence of anti-CD90 this was not the case, which may also indicate that the effects of anti-CD90 may require some more time before being effective.

Previously, an in vitro antiproliferative effect of anti-CD90 mAb was reported in T-cell and B-cell lymphoma cell lines [41]. Although the exact mechanism through which anti-CD90 mAb exerts its effect is unknown, it was

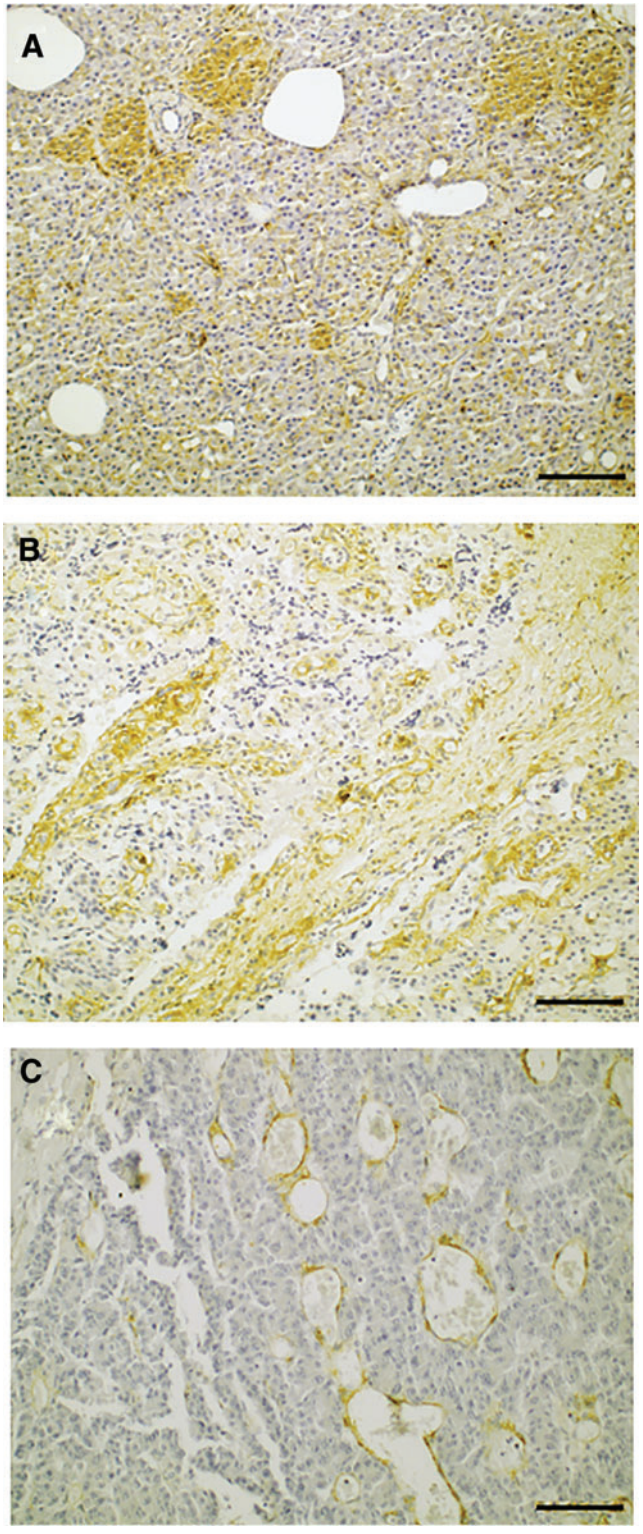


**FIG. 5.** CD90 immunohistochemistry of insulinomas. **(A)** Positive cytoplasmic tumor cell staining in focal areas. **(B)** Positive staining of intratumoral fibrous bands. **(C)** Positive staining of vascular endothelium. Color images available online at www.liebertpub.com/scd

demonstrated that anti-CD90 mAb induced apoptosis in murine T-lymphoma cells through caspase activation and downregulation of antiapoptotic bcl-2 family members [42]. Furthermore, anti-CD90 mAb induced both apoptosis and necrosis in B-cell lymphoma cells, and it has been suggested that anti-CD90 mAb also leads to arrest of the cell cycle, because a discrepancy was observed between the percentage of proliferation inhibition and the number of apoptotic or necrotic B-cell lymphoma cells [41]. We demonstrated for the first time that anti-CD90 mAb decreased cancer cell viability in an in vivo model, however, the underlying mechanism of this effect should be further investigated.

To study the protein expression of CD90 in human INS we have performed immunohistochemical staining on sections of 17 benign INS and three moderate-to-high malignant INS. Only a faint cytoplasmic staining of fibroblasts was found in normal pancreatic tissue, whereas no normal endocrine or exocrine pancreatic cells, or normal vascular endothelium stained positive for CD90, in accordance to what was previously reported by Zhu et al. [43]. Fifty-nine percent of the benign INS demonstrated CD90 positivity in tumor cells, whereas 80% demonstrated more intense CD90 staining in fibroblasts in comparison to the fibroblasts from normal pancreatic tissue. No positive vascular endothelium was found in the benign INS. Previously, it was reported that 2/10 benign islet cell tumors demonstrated positive CD90 staining in their tumor cells and fibroblasts [43]. However, because this former study focused on CD90 expression in PDAC, no differentiation within the group of islet cell tumors was made between INS, glucagonomas and gastrinomas, which could explain the difference in $CD90^+$ staining percentages found between their and our study. Interestingly, besides fibroblast and tumor cell CD90 positivity, in the two moderate-to-high malignant INS with vascular endothelium present on the section, intense CD90 positivity of the vascular endothelium was found. Zhu et al. [43] also stained four islet cell carcinomas in which they found a similar staining pattern, demonstrating $CD90^+$ tumor cells and fluorescent colocalization of CD90 and vascular endothelial marker CD31. Furthermore, they stained 183 PDAC samples and demonstrated that CD90 was significantly overexpressed in PDACs compared with normal pancreas, chronic pancreatitis, and benign islet tumors. Like in malignant islet cell carcinomas, CD90 expression was observed in cancer-associated fibroblasts (CAFs) (judged on costaining with CAF marker αSMA), vascular endothelial cells, and tumor cells. They concluded that $CD90^+$ CAFs might directly stimulate PDAC proliferation through provision of growth factors and cytokines, and that CD90 expression on vascular endothelium suggests that CD90 might play a role in PDAC angiogenesis. Although we did not costain our INS sections with a CAF marker, it seems likely that these CD90+ fibroblasts are indeed CAFs, since the staining intensity was more intense than in normal pancreatic fibroblasts. Furthermore, the presence of CAFs staining positive for αSMA in INS has been described in a Rip1Tag2 mouse model [44]. Therefore, CAFs might also directly stimulate INS proliferation and CD90 might play a role in INS angiogenesis. Therefore, future CD90 targeting in INS should not be limited to targeting CD90+ CSCs, but it should also be focused on targeting $CD90^+$ endothelial cells and CAFs, since those strategies might also inhibit INS proliferation.

Besides therapeutically targeting CD90, another more readily available application of anti-CD90 mAbs might be to use them as diagnostic tracers for imaging and monitoring progression of INS. Although in the majority of cases INS localization is accurately diagnosed with imaging modalities, and in 10%–27% of the cases, the exact location remains occult [45]. It is, however, essential to detect the exact tumor position before surgery, for example, to prevent too extensive pancreatic resection, or to see whether laparoscopic removal of INS would be feasible. Recently, it was demonstrated that CD90 could serve as such a diagnostic marker in PDAC [46].

## Acknowledgments

The BON-1 cell line was a kind gift from Dr. J.C. Thompson, Department of Surgery, University of Texas Medical Branch, Galveston, TX. The authors thank Dr. P. Pozzilli, Department of Diabetes and Metabolism, St. Bartholomew's Hospital, London, United Kingdom, for providing them with the CM cell line. The authors gratefully acknowledge the advice and technical assistance of B.E. Snaar-Jagalska, PhD and K.A.J. Braat, BSc regarding the zebrafish embryo xenograft experiments. This work was supported by an Agiko Stipend (# 95003580) provided by ZonMw, The Netherlands Organization for Health Research and Development.

Prior Conference Presentations

*Posters:*

- 2014 Veterinary Cancer Society (VCS)/Veterinary Society of Surgical Oncology (VSSO) Conference, Asheville, NC.
  *CD90, a novel therapeutic target for cancer stem cells in insulinomas*
- Keystone Symposium, Cancer and Stem Cells 2013, Banff, Canada.
  *CD90 is a potential marker for cancer stem cells in insulinomas*
- Veterinary Science Day 2013, Soesterberg, The Netherlands.
  *CD90, a marker for cancer stem cells in insulinomas?*

*Oral presentation:*

- European Society of Veterinary Oncology (ESVONC) Annual Congress 2015, Krakow, Poland.
  *Invited clinical abstract*: *Anti-CD90 antibodies provide a potential adjuvant therapy targeting cancer stem cells in insulinomas and breast cancer*

## Author Disclosure Statement

No competing financial interests exist.

## References

1. Mehrabi A, L Fischer, M Hafezi, A Dirlewanger, L Grenacher, MK Diner, H Fonouni, M Golriz, C Garoussi, et al. (2014). A systematic review of localization, surgical treatment options, and outcome of insulinoma. Pancreas 43:675–686.
2. Okabayashi T, Y Shima, T Sumiyoshi, A Kozuki, S Ito, Y Ogawa, M Kobayashi and K Hanazaki. (2013). Diagnosis and management of insulinoma. World J Gastroenterol 14:829–837.
3. Danforth DN, Jr., P Gorden and MF Brennan. (1984). Metastatic insulin-secreting carcinoma of the pancreas: clinical course and the role of surgery. Surgery 96:1934–1938.
4. Grama D, B Eriksson, H Martensson, B Cedermark, B Ahrén, A Kristoffersson, J Rastad, K Oberg and G Akerström. (1992). Clinical characteristics, treatment and survival in patients with pancreatic tumors causing hormonal syndromes. World J Surg 16:632–639.
5. Baccelli I and A Trumpp. (2012). The evolving concept of cancer and metastasis stem cells. J Cell Biol 198:281–293.
6. Visvader JE. (2011). Cells of origin in cancer. Nature 469:314–322.
7. Van der Meulen T and MO Huising. (2014). Maturation of stem cell-derived beta-cells guided by the expression of urocortin 3. Rev Diabet Stud 11:115–132.
8. Jiang FX and G Morahan. (2014). Pancreatic stem cells remain unresolved. Stem Cells Dev 23:2803–2812.
9. Mani SA, W Guo, M-J Liao, EN Eaton, A Ayyanan, AY Zhou, M Brooks, F Reinhard, CC Zhang, et al. (2008). The epithelial-mesenchymal transition generates cells with properties of stem cells. Cell 133:704–715.
10. Lan L, Y Luo, D Cui, BY Shi and W Deng. (2013). Epithelial-mesenchymal transition triggers cancer stem cell generation in human thyroid cancer cells. Int J Oncol 43:113–120.
11. Fendrich V, K Maschuw, J Waldmann, M Buchholz, J Rehm, TM Gress, DK Bartsch and A König. (2012). Epithelial-mesenchymal transition is a critical step in tumorgenesis of pancreatic neuroendocrine tumors. Cancers 4:281–294.
12. Grande E, J Capdevila, J Barriuso, L Antón-Aparicio and D Castellano. (2012). Gastroenteropancreatic neuroendocrine tumor cancer stem cells: do they exist? Cancer Metastasis Rev 31:47–53.
13. Regitinig P, E Spuller and H Denk. (2001). Insulinoma of the pancreas with insular-ductular differentiation in its liver metastasis—indication of a common stem-cell origin of the exocrine and endocrine components. Virchows Arch 438:624–628.
14. Buishand FO, J Kirpensteijn, AA Jaarsma, EJM Speel, M Kik and JA Mol. (2013). Gene expression profiling of primary canine insulinomas and their metastases. Vet J 197:192–197.
15. Sadanandam A, S Wullschleger, CA Lyssiotis, C Grötzinger, S Barbi, S Bersani, J Körner, I Wafy, A Mafficini, et al. (2015). A cross-species analysis in pancreatic neuroendocrine tumors reveals molecular subtypes with distinctive clinical, metastatic, developmental, and metabolic characteristics. Cancer Discov 5:1296–1313.
16. Yang ZF, DW Ho, MN Ng, CK Lau, WC Yu, P Ngai, PW Chu, CT Lam, RT Poon and ST Fan. (2008). Significance of CD90+ cancer stem cells in human liver cancer. Cancer Cell 13:153–166.
17. Tang KH, YD Dai, M Tong, YP Chan, PS Kwan, L Fu, YR Qin, SW Tsao, HL Lung, et al. (2013). A CD90(+) tumor-initiating cell population with an aggressive signature and metastatic capacity in esophageal cancer. Cancer Res 73: 2322–2332.
18. He J, Y Liu, T Zhu, J Zhu, F Dimeco, AL Vescovi, JA Heth, KM Murasko, X Fan and DM Lubman. (2012). CD90 is identified as a candidate marker for cancer stem cells in primary high-grade gliomas using tissue microarrays. Mol Cell Proteomics 11:M111 010744.
19. Lobba AR, MF Forni, AC Carreira and MC Sogayar. (2012). Differential expression of CD90 and CD14 stem cell markers in malignant breast cancer cell lines. Cytometry A 81:1084–1091.

20. Yan X, H Luo, X Zhou, B Zhu, Y Wang and X Bian. (2013). Identification of CD90 as a marker for lung cancer stem cells in A549 and H446 cell lines. Oncol Rep 30:2733–2740.
21. Saalbach A, A Wetzel, UF Haustein, M Stichterling, JC Simon and U Anderegg. (2005). Interaction of human Thy-1 (CD90) with the integrin alphavbeta3 (CD51/CD61): an important mechanism mediating melanoma cell adhesion to activated endothelium. Oncogene 24:6526–6532.
22. Brinkhof B, B Spee, J Rothuizen and LC Penning. (2006). Development and evaluation of canine reference genes for accurate quantification of gene expression. Anal Biochem 356:36–43.
23. Lawson ND and BM Weinstein. (2002). In vivo imaging of embryonic vascular development using transgenic zebrafish. Dev Biol 248:307–318.
24. Sabaawy HE, Azuma M, LJ Embree, HJ Tsai, MF Starost and DD Hickstein. (2006) TEL-AML1 transgenic zebrafish model of precursor B cell acute lymphoblastic leukemia. Proc Natl Acad Sci U S A 103:15166–15171.
25. Kunz PL. (2015). Carcinoid and neuroendocrine tumors: building on success. J Clin Oncol 33:1855–1863.
26. Russell WMS and RL Burch. (eds). (1959). *The Principles of Humane Experimental Techniques*. Methuen, London.
27. Herrera MB, S Bruno, S Buttiglieri, C Tetta, S Gatti, MC Deregibus, B Bussolati and G Camussi. (2006). Isolation and characterization of a stem cell population from adult human liver. Stem Cells 24:2840–2850.
28. Saalbach A, T Wetzig, UF Haustein and U Anderegg. (1999). Detection of human soluble Thy-1 in serum by ELISA. Fibroblasts and activated endothelial cells are a possible source of soluble Thy-1 in serum. Cell Tissue Res 298:307–315.
29. Ullah I, RB Subbarao and GJ Rho. (2015). Human mesenchymal stem cells—current trends and future prospective. Biosci Rep 35:e00191.
30. Vidal M, R Morris, F Grosveld and E Spanopoulou. (1990). Tissue-specific control elements of the Thy-1 gene. EMBO J 9:833–840.
31. Rege TA and JS Hagood. (2006). Thy-1 as a regulator of cell-cell and cell-matrix interactions in axon regeneration, apoptosis, adhesion, migration, cancer, and fibrosis. FASEB J 20:1045–1054.
32. Jiang J, Y Zhang, S Chuai, Z Wang, D Zheng, F Xu, Y Zhang, C Li, Y Liang and Z Chen. (2012). Trastuzumab (herceptin) targets gastric cancer stem cells characterized by CD90 phenotype. Oncogene 31:671–682.
33. Cheng BQ, Y Jiang, DL Li, JJ Fan and M Ma. (2012). Upregulation of thy-1 promotes invasion and metastasis of hepatocarcinomas. Asian Pac J Cancer Prev 13:1349–1353.
34. Chen WC, YS Chang, HP Hsu, MC Yen, HL Huang, CY Cho, CY Wang, TY Weng, PT Lai, et al. (2015). Therapeutics targeting CD90-integrin-AMPK-CD133 signal axis in liver cancer. Oncotarget 6:42923–42937.
35. Baroni MG, MG Cavallo, M Mark, L Monetini, B Stoehrer and P Pozzilli. (1999). Beta-cell gene expression and functional characterization of the human insulinoma cell line CM. J Endocrinol 161:59–68.
36. Evers BM, J Ishizuka, CM Townsend, Jr., and JC Thompson. (1994). The human carcinoid cell line, BON. A model system for the study of carcinoid tumors. Ann N Y Acad Sci 733:393–406.
37. Li J, H Liu, J Yu and H Yu. (2015). Chemoresistance to doxorubicin induces epithelial-mesenchymal transition via upregulation of transforming growth factor β signaling in HCT116 colon cancer cells. Mod Med Rep 12:192–198.
38. Pirozzi G, V Tirino, R Camerlingo, R Franco, A La Rocca, E Liguori, N Martucci, F Paino, N Normanno and G Rocco. (2011). Epithelial to mesenchymal transition by TGFβ-1 stemness characteristics in primary non small cell lung cancer cell line. PLoS One 6:e21548.
39. Beuran M, I Negoi, S Paun, AD Ion, C Bleotu, R Negoi and S Hostiuc. (2015). The epithelial to mesenchymal transition in pancreatic cancer: a systematic review. Pancreatology 15:217–225.
40. Lu H, KR Clauser, WL Tam, J Fröse, X Ye, EN Eation, F Reinhardt, VS Donnenberg, R Bhargava, SA Carr and RA Weinberg. (2014). A breast cancer stem cell niche supported by juxtacrine signalling from monocytes and macrophages. Nat Cell Biol 16:1105–1117.
41. Ishiura Y, N Kotani, R Yamashita, H Yamamoto, Y Kozutsumi and K Honke. (2010). Anomalous expression of Thy1 (CD90) in B-cell lymphoma cells and proliferation inhibition by anti-Thy1 antibody treatment. Biochem Biophys Res Commun 396:329–334.
42. Fujita N, Y Kato, M Naito and T Tsuruo. (1996). A novel anti-Thy-1 (CD90) monoclonal antibody induces apopotosis in mouse malignant T-lymphoma cells in spite of inducing bcl-2 expression. Int J Cancer 66:544–550.
43. Zhu J, S Thakolwiboon, X Liu, M Zhang and DM Lubman. (2014). Overexpression of CD90 (Thy-1) in pancreatic adenocarcinoma present in the tumor microenvironment. PLoS One 9:e115507.
44. Direkze NC, K Hodivala-Dilke, R Jeffery, T Hunt, R Poulsom, D Oukrif, MR Alison and NA Wright. (2004). Bone marrow contribution to tumor-associated myofibroblasts and fibroblasts. Cancer Res 64:8492–8495.
45. Abboud B and J Boujaoude. (2008) Occult sporadic insulinoma: localization and surgical strategy. World J Gastroenterol 14:657–665.
46. Foygel K, H Wang, S Machtaler, AM Lutz, R Chen, M Pysz, AW Lowe, L Tian, T Carrigan, TA Brentnall and JK Willmann. (2013). Detection of pancreatic ductal adenocarcinoma in mice by ultrasound imaging of thymocyte differentiation antigen 1. Gastroenterology 145:885–894.

Address correspondence to:
*Floryne O. Buishand, DVM, PhD*
*Department of Clinical Sciences of Companion Animals*
*Faculty of Veterinary Medicine*
*Utrecht University*
*Yalelaan 108*
*Utrecht 3584 CM*
*The Netherlands*

*E-mail:* f.o.buishand@uu.nl

Received for publication February 3, 2016
Accepted after revision April 4, 2016
Prepublished on Liebert Instant Online April 6, 2016